SCIENCE CHINA
Technological Sciences

•Article•

May 2024 Vol.67 No.5: 1567–1578
https://doi.org/10.1007/s11431-023-2637-1

Memristive oscillator to memristive map, energy characteristic

GUO YiTong[1,2], MA Jun[1,2,3*], ZHANG XiaoFeng[2] & HU XiKui[3]

[1] *College of Electrical and Information Engineering, Lanzhou University of Technology, Lanzhou 730050, China;*
[2] *Department of Physics, Lanzhou University of Technology, Lanzhou 730050, China;*
[3] *School of Science, Chongqing University of Posts and Telecommunications, Chongqing 400065, China*

Received December 22, 2023; accepted March 12, 2024; published online April 22, 2024

Most of nonlinear oscillators composed of capacitive and inductive variables can obtain the Hamilton energy by using the Helmholtz theorem when the models are rewritten in equivalent vector forms. The energy functions for biophysical neurons can be obtained by applying scale transformation on the physical field energy in their equivalent neural circuits. Realistic dynamical systems often have exact energy functions, while some mathematical models just suggest generic Lyapunov functions, and the energy function is effective to predict mode transition. In this paper, a memristive oscillator is approached by two kinds of memristor-based nonlinear circuits, and the energy functions are defined to predict the dependence of oscillatory modes on energy level. In absence of capacitive variable for capacitor, the physical time t and charge q are converted into dimensionless variables by using combination of resistance and inductance (L, R), e.g., $\tau=t\times R/L$. Discrete energy function for each memristive map is proposed by applying the similar weights as energy function for the memristive oscillator. For example, energy function for the map is obtained by replacing the variables and parameters of the memristive oscillator with corresponding variables and parameters for the memristive map. The memristive map prefers to keep lower average energy than the memristive oscillator, and chaos is generated in a discrete system with two variables. The scheme is helpful for energy definition in maps, and it provides possible guidance for verifying the reliability of maps by considering the energy characteristic.

Hamilton energy, memristor, Helmholtz theorem, scale transformation, memristive circuit

Citation: Guo Y T, Ma J, Zhang X F, et al. Memristive oscillator to memristive map, energy characteristic. Sci China Tech Sci, 2024, 67: 1567–1578, https://doi.org/10.1007/s11431-023-2637-1

1 Introduction

Nonlinear circuits are often used as signal sources and further filtering of the output signals can match with some realistic signals within specific frequency band. High order nonlinear terms account for complexity and specific function in electric components, which are crucial for supporting chaotic states and field energy savage. By taming some intrinsic parameters, chaos and hyperchaos are induced in the nonlinear circuits [1–4], which are often described by equivalent nonlinear oscillators, and these chaotic systems have potential application in image encryption [5–8]. The bionics throws light on the achievements of artificial intelligence [9,10] and functional enhancements of artificial neurons and setting on biophysical neurons [11–15]. For further clues about model approach of neural activities from physical aspect, readers can explore suggestions in the recent review and the references therein [16].

The reliability of nonlinear circuits depends on the controllability. It means that most of the intrinsic parameters can be controllable in wide range. External stimuli accompanying with energy injection can be encoded to guide the outputs to reach target levels. The cell membrane and synapse of a biological neuron have distinct flexibility, as a result, gradient energy and external stimuli including forcing current, depolarized field will change the energy level and firing

*Corresponding author (email: hyperchaos@163.com)

modes in neural activities in adaptive way. Therefore, the synaptic intensity is regulated under the energy flow [17,18]. For example, an adaptive law [17,18] is suggested to control the growth of synaptic intensity in two kinds of memristive neurons, which are developed from neural circuits connecting with memristive channels. Furthermore, two or more neurons can be connected by synapses with a growth of the synaptic intensity until reaching energy balance, while heterogeneity [19,20] can be created in the neural network due to continuous energy collection from the adjacent neurons.

Most of the nonlinear circuits can present periodic or chaotic states. A few nonlinear circuits can be tamed to present similar firing patterns derived from biological neurons. Some neural circuits are designed and their dimensionless forms are used as neuron models [21–25]. It is crucial to consider the physical property of biological neurons before building an equivalent simple neural circuit. Static distribution of intracellular ions induces electric field in the cell membrane, stochastic diffusion and propagation of ions across the cell membrane induce magnetic field due to current effect. Continuous exchange of energy flow will change the distribution of intracellular and extracellular ions, and thus the relation between membrane potential and channel current becomes nonlinear dependence. Therefore, capacitor, inductor, nonlinear resistor and constant voltage source are four necessary elements for building a simple neural network. The capacitor accounts for the capacitive property of cell membrane, an inductor mimics the magnetic field effect because of propagation and diffusion of ions, constant voltage results from the resting potential in an ion channel. In a neural circuit, a constant voltage source is often connected to the inductor in series, and the nonlinear resistor is used as additive channel to shunt energy flow. When piezoelectric ceramics, phototube and thermistor are incorporated into the neural circuit, the neurons become sensitive to external voice, illumination and temperature [26–30]. In particular, the involvement of memristive current and magnetic flux variable into the neuron models can estimate the electromagnetic induction and radiation [31–35]. Based on these memristive neurons, the collective neural activities can be controlled under field coupling even synaptic coupling is suppressed greatly.

Oscillator-like models can be derived from circuit equations by applying scale transformation on the physical variables and parameters in the neural circuits. The energy function composed of capacitive, inductive and memristive terms can be mapped from the field energy for the electric components with distinct field effect including capacitor, inductor and memristor. The energy function can also be derived and verified by using the Helmholtz theorem when the formulas for the neuron model are updated with vector forms. The emergence of chaos in an autonomous oscillator requires involvement of three variables at least in absence of noisy disturbance and time delay. However, a map can produce chaotic series even one variable is regulated. To produce chaotic behaviour in the neural activities, three-variable neurons and two-variable models driven by external periodic current in the form of nonlinear oscillators have been investigated extensively. However, discrete systems and maps (discrete neurons) [36–38] are effective to mimic the main firing modes in some biological neurons, and the involvement of memristive term is helpful to estimate the electromagnetic induction as well [39,40]. Memsitor shows great application in neural circuits and synapse implement for neuromorphic computing see recent review works [41–44]. Most of the memristive oscillators can be approached by setting equivalent memristor-based circuits and the energy characteristic is clear. However, many works about discrete memristor and memristive maps are discussed from mathematical definition and field programmable gate array (FPGA) simulation [39,45–49], and how to describe the energy characteristic keeps open. Therefore, it is a challenge to define and estimate the energy function for map neurons, and the energy level dependence on firing modes keeps open.

In this paper, a memristive oscillator is expressed by two different kinds of nonlinear circuits coupled by magnetic flux-controlled memristor (MFCM) and charge-controlled memristor (CCM), respectively. CCM and a voltage-controlled element are used to couple the inductor when capacitor is not available. After scale transformation, two kinds of memristor-based circuits are described by similar memristive oscillators and energy functions are defined. Applying linear transformation on the variables and intrinsic parameters, each memristive oscillator is replaced by a memristive map under covariation. For example, $\mathrm{d}y/\mathrm{d}t=A\times y(1-y)$ to $x_{n+1}=B\times x_n(1-x_n)$. Then the energy function for the memristive oscillator is referred to define a discrete energy function for the map with the same weights. Bifurcation analysis is carried out, and the average energy is calculated to predict coherence resonance in the memristive maps.

2 Model and scheme

Reliable algorithm is crucial to obtain numerical solutions for nonlinear equations, e.g., the fourth order Runge-Kutta algorithm is effective to find solve numerical results for nonlinear oscillators described by differential equations, which are often discretized in exact forms. In particular, the involvement of noisy excitations and disturbances makes a stochastic dynamical system, and the approach of numerical results depends on reliable algorithms [50,51]. On the other hand, map modelling of complex systems can avoid and reduce the difficulty during numerical approach. In ref. [52], energy function for memristive devices is defined and estimation of energy for some maps is discussed. It is assumed

that the same weights can be applied for the energy function of a map by exploring the Hamilton energy function for an equivalent nonlinear oscillator, which has distinct covariation with the map. In ref. [53]. linear transformation is applied to bridge connection to two nonlinear oscillators and their equivalent maps. The capacitive energy $0.5C\times V^2$ for a capacitor and inductive energy $0.5L\times i^2$ for an inductor can be mapped into equivalent forms as $0.5A\times x^2$ and $0.5B\times y^2$, where V, i are physical variables, x, y are corresponding dimensionless variables, and A, B are normalized gains for the energy terms. Both MFCM [54–56] and CCM [57–59] can save and contain field energy when they are incorporated into a linear or nonlinear circuit. The energy property in an MFCM and CCM can be described by suitable energy function in an equivalent inductor and capacitor, respectively. In fact, the energy description for memristive devices often presents a high order term. That is, scale transformation bridges connection between the circuit equations and the nonlinear oscillator, field energy and Hamilton energy completely [60].

For a nonlinear oscillator with a few variables, the dynamics can be investigated in its equivalent nonlinear circuit. It is a challenge to verify the numerical results during selecting and combining these potential electric components. For example, the variables (x, y, z, …) for a nonlinear oscillator can be described by the output voltage for a capacitor, induction current along an induction coil, and a constant term often means involvement of constant voltage source in the branch circuit. Is it possible to build more equivalent nonlinear circuits for mimicking the dynamics for the same nonlinear oscillator? From physical viewpoint, continuous oscillation in a nonlinear circuit requires the involvement of capacitive and inductive components synchronously. In ref. [53], the author suggested a memristive oscillator with two variables, and scale transformation is applied to obtain an equivalent map for further energy estimation.

2.1 Linear transformations between memristive oscillator and memristive map

The memristive oscillator is given in the form as follows:

$$\begin{cases} \dfrac{\mathrm{d}y}{\mathrm{d}\tau} = ry(1-y)-(\alpha'+3\beta'\varphi'^2)y, \\ \dfrac{\mathrm{d}\varphi'}{\mathrm{d}\tau} = a\varphi'+by, \end{cases} \tag{1}$$

where r, a, b, α', β' are dimensionless parameters, and y, φ' are dimensionless variables. Indeed, the eq. (1) is autonomous and it seldom presents chaotic series without external stimulus or noisy disturbance. The Hamilton energy for the memristive oscillator is described by

$$H = \frac{1}{2}y^2+\frac{1}{2}(\alpha'\varphi'+3\beta'\varphi'^3)y. \tag{2}$$

When the variable y is mapped from a voltage variable, the two energy terms are relative to capacitive and memristive field, respectively. By applying the following linear transformation in eq. (3), the memristive oscillator in eq. (1) is replaced by a memristive map with similar form in discrete type in eq. (4).

$$\begin{cases} \lambda = 1+r\Delta\tau,\ \alpha' = \dfrac{\alpha}{\varepsilon},\ \beta' = \dfrac{\beta\Delta\tau r^2}{(1+r\Delta\tau)^2}, b = \dfrac{\varepsilon}{\Delta\tau}, \\ \varphi_n = \dfrac{r\Delta\tau}{(1+r\Delta\tau)}\varphi'_n,\ x_n = \dfrac{r\Delta\tau}{1+r\Delta\tau}y_n,\ a = \dfrac{(k-1)}{\Delta\tau}, \end{cases} \tag{3}$$

where the variables (yn, $\varphi n'$) are sampled time series for the variables (y, φ') in eq. (1), $\Delta\tau$ is the time step for numerical approach of eq. (1).

$$\begin{cases} x_{n+1} = \lambda x_n(1-x_n)-(\alpha+3\beta\varphi_n^2)x_n, \\ \varphi_{n+1} = k\varphi_n+\varepsilon x_n. \end{cases} \tag{4}$$

The memristive map in eq. (4) can be regulated in the parameters for developing different firing patterns. The memristive oscillator in eq. (1) can be verified by designing two equivalent circuits by incorporating different memristors. Case 1: Capacitor, nonlinear resistor and MFCM are connected in the neural circuit. Case 2: Inductor, a voltage-dependent element and CCM are connected in the neural circuit.

2.2 Approach of memristive oscillator by using MFCM

To verify the reliability of eq. (1), a nonlinear circuit in Figure 1 is plotted to match with the energy property in eq. (2). It is helpful to predict the physical properties of electric components involved in this circuit.

The channel current i_{NR} across the nonlinear resistor and memristive current i_{M} are respectively described by [60]

$$\begin{cases} i_{\mathrm{NR}} = -\dfrac{r}{\rho}(V-\dfrac{V^2}{V_0}); \\ i_{\mathrm{M}} = \dfrac{\mathrm{d}q}{\mathrm{d}t} = M(\phi)V = (\alpha_1+3\beta_1\phi^2)V, \end{cases} \tag{5}$$

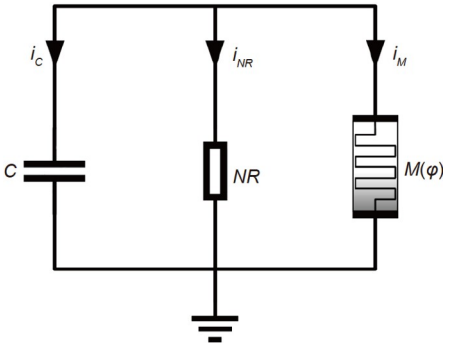

Figure 1 Schematic diagram for a neural circuit coupled by MFCM. A memristive circuit composed of one capacitor, nonlinear resistor (NR) and one MFCM.

where V estimates the output voltage for the capacitor with capacitance C, ϕ is the magnetic flux variable across the memristor with physical parameters (α, β). V_0 is constant, and the gains (r, b) are the same parameters in eq. (1). Under the Kirchhoff's theorem, the relations between physical variables for Figure 1 are defined by

$$\begin{cases} C\dfrac{\mathrm{d}V}{\mathrm{d}t} = -i_{\mathrm{NR}} - i_{\mathrm{M}}, \\ \dfrac{\mathrm{d}\phi}{\mathrm{d}t} = A\phi + bV, \end{cases} \tag{6}$$

where the normalized parameter b has no physical unit, and the parameter A has physical unit. The physical variables and parameters in eq. (6) are rewritten in a dimensionless form [61]:

$$\begin{cases} y = \dfrac{V}{V_0},\ \varphi' = \dfrac{\phi}{\rho C V_0}, \tau = \dfrac{t}{\rho C}, \\ \alpha' = \rho\alpha_1, \beta' = \rho^3 C^2 V_0^2 \beta_1, a = A\rho C. \end{cases} \tag{7}$$

Inserting the variables and parameters for eq. (7) into the eq. (6), it has the same form as presented in eq. (1). That is, eq. (6) can produce similar behaviors in the memristive oscillator in eq. (1). The capacitive and memristive energy W_1 and the dimensionless form for eq. (6) are estimated by [61]

$$\begin{cases} W_1 = \dfrac{1}{2}CV^2 + \dfrac{1}{2}L_{\mathrm{M}} i_{\mathrm{M}}^2 = \dfrac{1}{2}CV^2 + \dfrac{1}{2}\phi i_{\mathrm{M}}, \\ H_1 = \dfrac{W_1}{CV_0^2} = \dfrac{1}{2}y^2 + \dfrac{1}{2}(\alpha'\varphi' + 3\beta'\varphi'^3)y. \end{cases} \tag{8}$$

That is, the field energy in eq. (8) is consistent with the energy description in eq. (2), and the Hamilton energy is verified by using the Helmholtz theorem when the memristive oscillator is rewritten in a vector form. Therefore, combination of a capacitor and an MFCM accompanying with a nonlinear resistor is effective to reproduce similar dynamical behaviors in the nonlinear oscillator in eq. (1). The potential mechanism is that continuous oscillation in nonlinear system requires continuous exchange between capacitive and inductive field.

2.3 Approach of memristive oscillator by using CCM

A CCM has similar physical property as capacitor by keeping capacitive property in field and energy characteristic. It is interesting to investigate whether combination of inductor and CCM can develop similar dynamics in eq. (1), and the circuit implement is plotted in Figure 2.

According to Figure 2, the dimensionless variables (y, φ') in eq. (1) can link to the channel current across the inductor and charge for the CCM. The relation between variables in Figure 2 is defined as follows:

$$\begin{cases} L\dfrac{\mathrm{d}i_L}{\mathrm{d}t} = V_{i_L} - V_{\mathrm{M}}, \\ \dfrac{\mathrm{d}q}{\mathrm{d}t} = Bq + di_L. \end{cases} \tag{9}$$

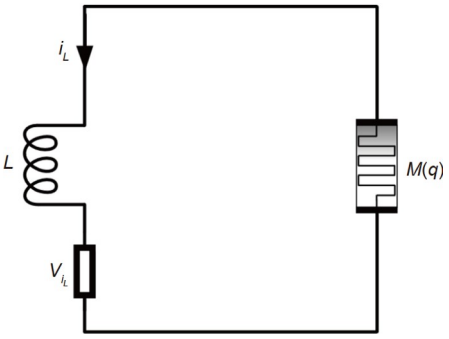

Figure 2 Schematic diagram for a neural circuit coupled by CCM. A memristive circuit connected by one inductor, nonlinear resistor (NR) and one CCM.

The parameter B is relative to the physical property of the CCM, and it is approached by $B=\sigma/C_0$, which C_0 measures the capacitive ability in the CCM and σ is a constant conductance. The physical characteristic for the CCM and channel current for NR are defined by

$$\begin{cases} V_{i_L} = \rho\left(i_L - \dfrac{\rho i_L^2}{V_0}\right), \\ V_{\mathrm{M}} = M(q)i_L = (\alpha_2 + 3\beta_2 q^2)i_L. \end{cases} \tag{10}$$

By applying similar scale transformation for the variables and parameters in eqs. (9) and (10), a group of new variables and parameters are obtained by

$$\begin{cases} z' = \dfrac{\rho i_L}{V_0},\ q' = \dfrac{q}{C_0 V_0},\ \tau = \dfrac{t}{\rho C_0}, \gamma = \dfrac{\rho^2 C_0}{L}, \\ \alpha' = \dfrac{\rho C_0}{L}\alpha_2, \beta' = \dfrac{\rho C_0^3 V_0^2}{L}\beta_2, c = \sigma\rho. \end{cases} \tag{11}$$

As a result, the eq. (9) is updated in a dimensionless form as follows:

$$\begin{cases} \dfrac{\mathrm{d}z'}{\mathrm{d}\tau} = \gamma z'(1 - z') - (\alpha' + 3\beta' q'^2)z', \\ \dfrac{\mathrm{d}q'}{\mathrm{d}\tau} = cq' + dz'. \end{cases} \tag{12}$$

It has the identical form shown in eq. (1) even the symbols for variables and parameters show some differences. Therefore, the two memristive systems in eqs. (1) and (12) can present similar oscillatory characteristic by applying suitable parameters. It is important to identify the energy for the nonlinear circuit in Figure 2 and the field energy and its dimensionless energy form are given in

$$\begin{cases} W_2 = \dfrac{1}{2}Li_L^2 + \dfrac{1}{2}C_{\mathrm{M}}V_{\mathrm{M}}^2 = \dfrac{1}{2}Li_L^2 + \dfrac{1}{2}qV_{\mathrm{M}}, \\ H_2 = \dfrac{W_2}{C_0 V_0^2} = \dfrac{1}{2\gamma}z'^2 + \dfrac{1}{2\gamma}(\alpha' q' + 3\beta' q'^3)z'. \end{cases} \tag{13}$$

By using similar linear transformation, the dynamics in eq. (12) can be presented in a map form.

$$\begin{cases} w_{n+1} = \eta w_n(1 - w_n) - (\alpha + 3\beta q_n^2)w_n, \\ q_{n+1} = \delta q_n + \mu w_n. \end{cases} \tag{14}$$

From eq. (12) to eq. (14), it requires the following criterion for redefining the parameters and variables.

$$\begin{cases} \eta = 1+\gamma\Delta\tau,\ \alpha' = \dfrac{\alpha}{\Delta\tau},\ \beta' = \dfrac{\beta\Delta\tau\gamma^2}{(1+\gamma\Delta\tau)^2}, d = \dfrac{\mu}{\Delta\tau}, \\ q_n = \dfrac{\gamma\Delta\tau}{(1+\gamma\Delta\tau)} q'_n,\ w_n = \dfrac{\gamma\Delta\tau}{1+\gamma\Delta\tau} z'_n,\ c = \dfrac{\delta-1}{\Delta\tau}, \end{cases} \tag{15}$$

where the variables (z'_n, q_n') are discretized from the variables (z', q') in eq. (12). Both eqs. (4) and (14) have the similar form even these dimensionless variables are mapped from different physical variables. However, their energy functions in eqs. (8) and (13) are much different because the physical field energy can be kept in different types. It means that combination of different electronic components will have different energy thresholds and ranges. Indeed, circuit implement of the same nonlinear oscillator is dependent on the combination of electric components greatly. A capacitive component is crucial to keep electric field, and then discharge will pump energy into inductive components for inducing continuous oscillation. When a capacitor is not available, a CCM is effective to save and propagate charges in continuous way. As a result, changes of the channel current passed in the inductor or induction coil generate an induced electromotive force. Therefore, capacitive components are indispensable elements to build nonlinear circuits, and specific component dependent on charge flow similar as the form of eq. (10) becomes indispensable.

2.4 Scale transformation for physical parameters and units

In generic way, standard physical time unit is available when both intrinsic parameters including capacitance and resistance (C, R) or capacitive and inductance (C, L) are known, and then the physical time is converted into dimensionless time variable as $\tau=t/RC$, or $\tau=t/(LC)^{1/2}$. In fact, when the intrinsic parameter C is not known, another time factor can be used as reference value

$$\begin{cases} \eta = 1+\gamma\Delta\tau,\ \alpha' = \dfrac{\alpha}{\Delta\tau},\ \beta' = \dfrac{\beta\Delta\tau\gamma^2}{(1+\gamma\Delta\tau)^2}, d = \dfrac{\mu}{\Delta\tau}, \\ q_n = \dfrac{\gamma\Delta\tau}{(1+\gamma\Delta\tau)} q'_n,\ w_n = \dfrac{\gamma\Delta\tau}{1+\gamma\Delta\tau} z'_n,\ c = \dfrac{\delta-1}{\Delta\tau}. \end{cases} \tag{16}$$

Therefore, replacing the variables in eq. (9) can develop the memristive circuit in another form without clarifying $B=\sigma/C_0$. A group of new variables and parameters are defined by

$$\begin{cases} z' = \dfrac{\rho i_L}{V_0},\ q' = \dfrac{\rho^2}{LV_0} q,\ \tau = \dfrac{\rho t}{L}, \\ \alpha' = \dfrac{1}{\rho}\alpha_2, \beta' = \dfrac{L^2V_0^2}{\rho^5}\beta_2, k_2 = \dfrac{BL}{\rho}. \end{cases} \tag{17}$$

The memristive circuit in eq. (9) is updated with a new form as follows:

$$\begin{cases} \dfrac{\mathrm{d}z'}{\mathrm{d}\tau} = z'(1-z') - (\alpha' + 3\beta' q'^2) z', \\ \dfrac{\mathrm{d}q'}{\mathrm{d}\tau} = k_2 q' + dz'. \end{cases} \tag{18}$$

It presents similar form as shown in eq. (12). As a result, similar dynamics can be reproduced by taming the parameters in eq. (18). As a result, similar discrete system for eq. (18) can be obtained in the form as presented in eq. (14). The energy function for eq. (18) is given in the form as follows:

$$\begin{cases} W_3 = \dfrac{1}{2}Li_L^2 + \dfrac{1}{2}C_{\mathrm{M}}V_{\mathrm{M}}^2 = \dfrac{1}{2}Li_L^2 + \dfrac{1}{2}qV_{\mathrm{M}}, \\ H_3 = \dfrac{W_2}{V_0^2(L/\rho^2)} = \dfrac{W_2\rho^2}{LV_0^2} = \dfrac{1}{2}z'^2 + \dfrac{1}{2}(\alpha' q' + 3\beta' q'^3) z'. \end{cases} \tag{19}$$

Indeed, scale transformation seldom changes the energy function for the memristive circuit. Therefore, eq. (18) has the same form of energy function defined in eq. (13) accompanying the gain $p=1/\gamma$. It is interesting to discuss the energy approach for the memristive maps in possible way. Eq. (8) presents exact calculation of energy for the memristive eq. (1). Considering relation between these parameters for the oscillator and map, a discrete energy function for eq. (4) is estimated as follows:

$$H_n' = \frac{1}{2}x_n^2 + \frac{1}{2}(\alpha\varphi_n + 3\beta\varphi_n^3)x_n. \tag{20}$$

For the memristive map in eq. (14), the energy function is suggested as follows:

$$H_n'' = p[\frac{1}{2}w_n^2 + \frac{1}{2}(\alpha q_n + 3\beta q_n^3)w_n]\ . \tag{21}$$

The weight or gain for the energy function in eq. (14) can be selected with $p=1$, and it has no distinct impact on the exchange between capacitive and inductive energy terms. The discrete energy function in eq. (21) is consistent with a discrete form from eq. (19), and it indicates that the dimensionless energy function is independent of the scale transformation because the energy function can be mapped from the sole field energy function for the memristive circuit completely.

Appearance and emergence of chaos in an autonomous nonlinear oscillator requires three variables at least. In absence of external periodic forcing or noisy excitation, the memristive oscillator in eqs. (1), (12), (18) just contains two variables. Therefore, periodic oscillatory states can be developed rather than inducing any chaotic series. As is known, chaos can be induced one-variable map and two-variable map. Therefore, the memristive maps shown in eqs. (4) and (14) can be tamed to present chaotic states by setting appropriate values for the dimensionless parameters for supporting a positive Lyapunov exponent. The potential mechanism is that the discretization operation for the nonlinear oscillators introduces time factor for the variables into the new developed maps, and the sampled time series in

periodic type are encoded in the amplitude and interval synchronously. Therefore, these mapped discrete systems can present chaos or new periodic characteristic. In this case, the memristive maps have distinct advantage than the memristive oscillators for producing similar firing activities as biological neurons.

2.5 Adaptive growth law controlled by energy level

Biological neurons often show controllable properties during the polarization and magnetization, and even shape deformation is induced by specific mechanical stimuli. As a result, some intrinsic parameters for ion channel, capacitive and inductive properties are changed. Indeed, we can use a similar control law as in refs. [17,18] for the memristive parameters in eqs. (1), (12) and (18), and then the memristive oscillators can experience different firing modes and the average value for the energy function will show corresponding jump between different energy levels. To keep the same form for variables, the growth of intrinsic parameter is controlled with exponential form smoothly. For maps, the growth criterion is considered as saturation form restricted by a Heaviside function. For simplicity, we consider the adaptive growth of one memristive parameter for the memristive map as follows:

$$\begin{cases} \alpha = \alpha_0 + \Delta\alpha \cdot \mathrm{int}\left(\dfrac{n}{N_0}\right)\vartheta(H_n - \kappa), \\ \vartheta(P) = 1, P \geqslant 0, \vartheta(P) = 0, P < 0, \end{cases} \tag{22}$$

where α_0 is the initial value for memristive parameter, $\Delta\alpha$ is the growth step, n denotes iterations, N_0 measures the interval for next growth, κ is the energy threshold and the Heaviside function in eq. (22) controls its growth when the energy level is beyond a threshold. On the other hand, average energy value often predicts high regularity in the neural activities. Adaptive reduction in some parameters is also effective to control the mode transition. For example,

$$\begin{cases} \alpha = \alpha_0 - \Delta\alpha \cdot \mathrm{int}\left(\dfrac{n}{N_0}\right)\vartheta(\kappa - H_n), \\ \vartheta(P) = 1, P \geqslant 0, \vartheta(P) = 0, P < 0. \end{cases} \tag{23}$$

In the next section for numerical approach, the case defined in eq. (22) will be discussed. $\Delta\alpha>0$ means positive growth of the memristive parameter from a small value, $\Delta\alpha<0$ can calculate the case for reduction of memristive parameter from a high value.

3 Results and discussion

The memristive neuron can be presented in similar form in eqs. (1), (12) and (18) and parameters can be adjusted to trigger similar dynamical behaviors. The fourth order Runge-Kutta algorithm can be applied to explore the dynamics by finding the numerical solutions for the memristive oscillator even different symbols are used for the variables and parameters. Bifurcation parameters are changed to present different firing patterns, and the corresponding energy function is calculated as well. Our main aim is to investigate the dynamics and energy characteristic of the memristive map, and nonlinear response under the suggested adaptive law in eq. (23). At first, we calculated the mode selection in eq. (4) by changing one parameter carefully, and the distribution of variable series is plotted in Figure 3.

From Figure 3, it is demonstrated that the memristive map shows distinct transition between different firing modes by changing one intrinsic parameter carefully. Complete firing patterns including spiking, bursting and chaotic states are induced by taming a single parameter in continuous way. To discern the dynamics and energy characteristic of this memristive oscillator, formation of attractors and energy evolution are plotted for the neuron presenting different neural activities in Figure 4.

The profile of the attractor is relative to the firing mode and energy level. From chaotic state to periodic firing patterns, chaotic attractor is suppressed and the average energy value is increased. The similar case for memristive map in eq. (14) is explored, and the bifurcation diagram is plotted in Figure 5.

Complete firing modes are found in the memristive map in eq. (14) by adjusting one normalized parameter carefully,

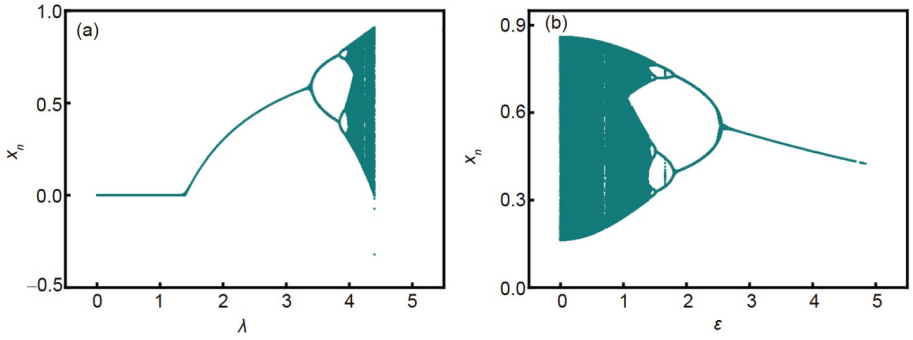

Figure 3 Bifurcation diagram of X_n vs. parameter λ (a) and parameter ε (b). (a) ε=0.15; (b) λ=4.2. Setting parameters α=0.4, β=0.02, k=0.5 and initials (0.2, 0.1).

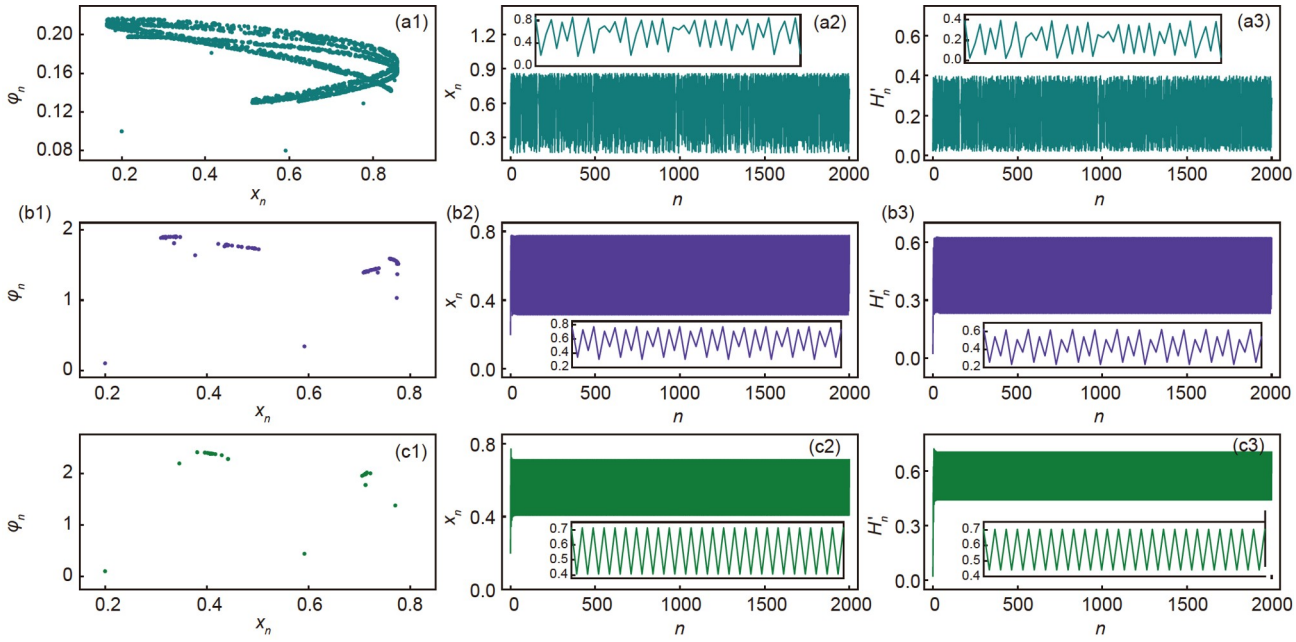

Figure 4 Developed attractors, evolution of variable x_n and energy level. (a1, a2, a3) ε=0.15; (b1, b2, b3) ε=1.45; (c1, c2, c3) ε=1.95. The other parameters are fixed at λ=4.2. (a3) $<H_n'>$=0.214; (b3) $<H_n'>$=0.435; (c3) $<H_n'>$=0.572. The enlarged images show the situation with iterations between 500 and 550.

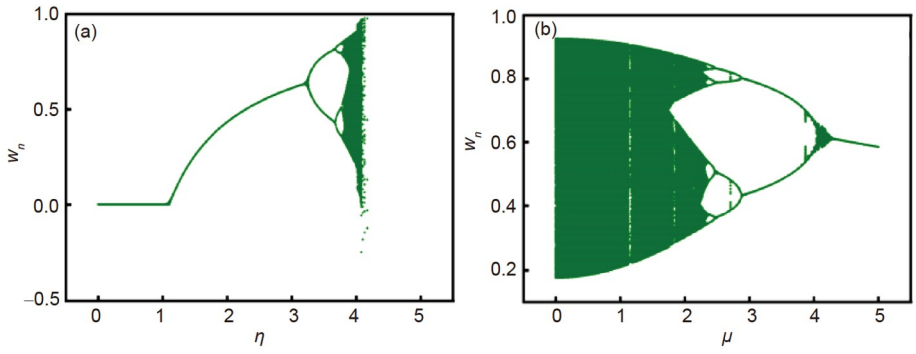

Figure 5 Bifurcation of variable W_n vs. parameter η (a) and parameter μ (b). (a) μ=1.75; (b) η=3.9. Setting parameters α=0.1, β=0.01, and δ=0.3.

and the mode transition in Figure 5 is some different from the distribution in eq. (3). Furthermore, the formation of attractor, changes of variable and energy function for the map are calculated in Figure 6. Shift in the average energy and changes of attractor profile predict mode transition in the memristive map.

By changing a single parameter in eq. (14), chaotic attractor is guided to show periodic type, and the average energy for the map also shows slight increase. Furthermore, it is interesting to discuss the formation of attractors and mode transition when the memristive map neuron in eq. (14) is regulated by the adaptive law in eq. (22), and changes of attractors are shown in Figure 7. Form simplicity, α_0=0.1, $\Delta\alpha$=0.005, κ=0.5, N_0=40 are used for the control law and map attractors are presented.

The shape of attractors is changed with adaptive growth of one memristive parameter in the map, chaotic and periodic attractors can be formed as well. For better clarification, the transition in the membrane potential, energy level and growth of memristive parameter is shown in Figure 8.

Distinct changes are observed in the series for membrane potential and energy function during the growth of memristive parameter with constant footstep. Similar to the growth criterion in eq. (22), one memristive parameter can be regulated with negative growth in eq. (23), which begins from a higher value to a lower value. Similar mode transition can be detected. By changing other parameters with the same control low, similar mode transition and jump between energy levels can be found as well.

By setting higher value for the gain $\Delta\alpha$ or smaller interval N_0, the memristive parameter encounters rapid growth and mode transition becomes more distinct. Furthermore, the case for μ=1.58, 2.85 is calculated in Figures 9 and 10.

From Figure 8 to Figure 10, the average energy is increased from 0.142 to 0.607, and the firing mode is also switched from chaotic to periodic oscillation. For most of the

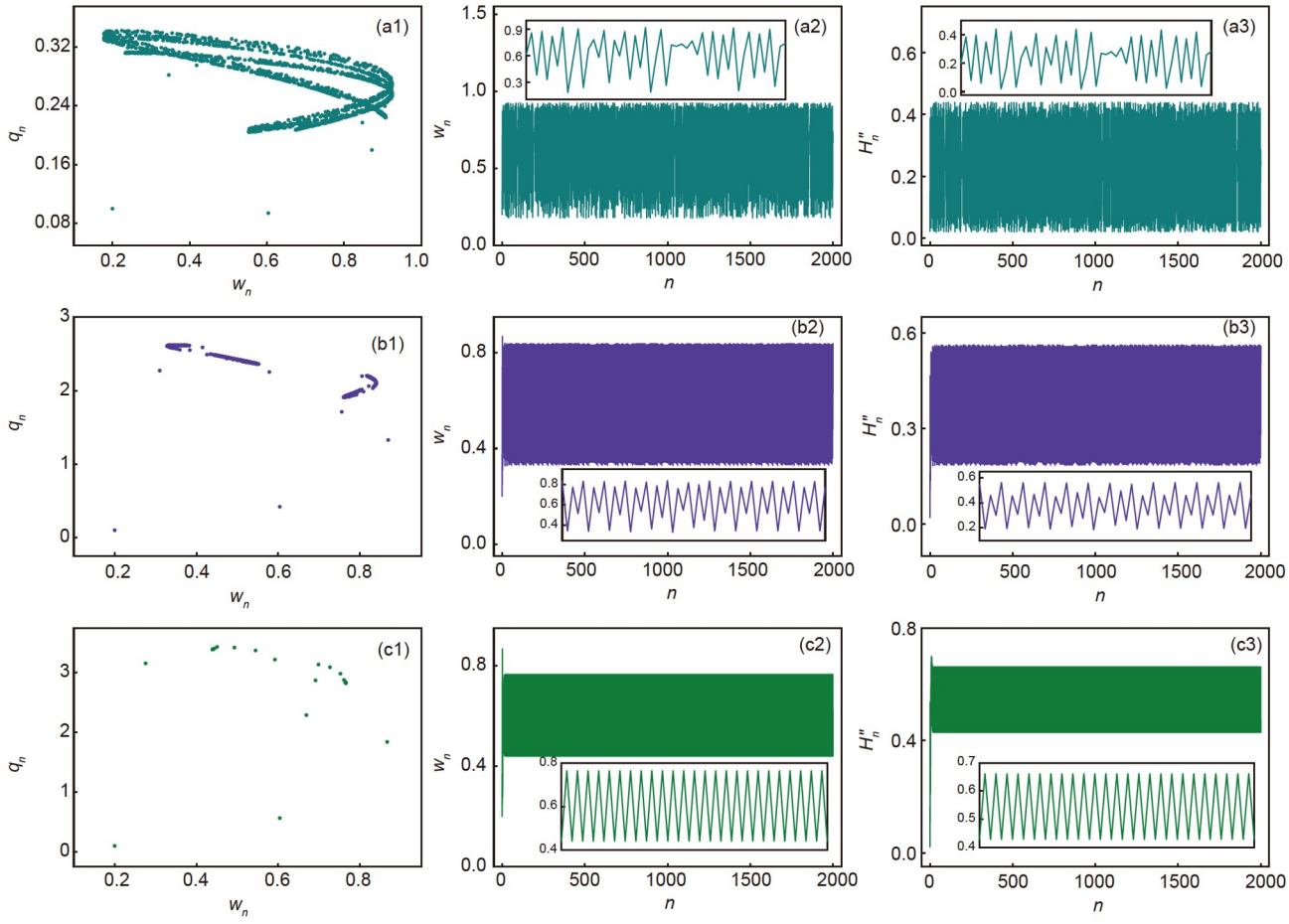

Figure 6 Developed attractors, evolution of variable w_n and energy level. (a1, a2, a3) μ=0.22; (b1, b2, b3) μ=1.85; (c1, c2, c3) μ=2.58. Setting parameters η=3.9, p=1. The average energy for (a3) $<H_n''>$=0.233, (b3) $<H_n''>$=0.379, (c3) $<H_n''>$=0.544. Enlarged images show the situation with iterations between 500 and 550.

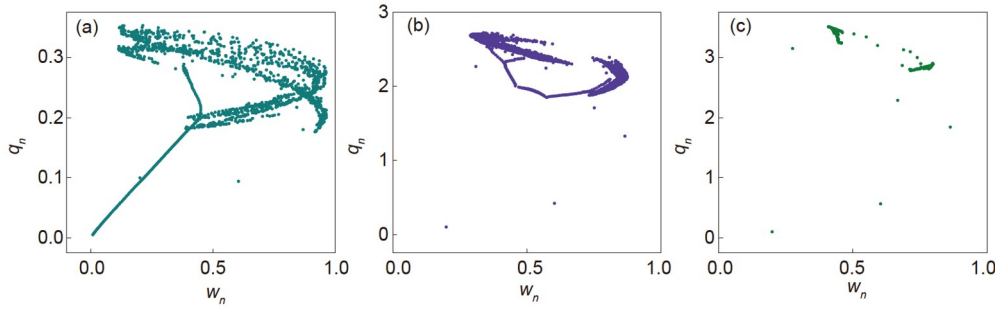

Figure 7 Developed attractors by changing parameter μ. (a) μ=0.22; (b) μ=1.85; (c) μ=2.58. Setting parameters α_0=0.1, $\Delta\alpha$=0.005, κ=0.5, N_0=40, β=0.01, η=3.9, and the initial values select (0.2, 0.1).

neuron models, the distributions of peak value, interspike intervals (ISI), discrete variable vs. bifurcation parameter seldom show continuous changes, and the firing modes in neural activities are modified when one parameter is changed continuously. That is, one bifurcation parameter can select different values to support the same firing activities such as chaotic, periodic spiking and bursting, and quiescent state. By extensive approach the average Hamilton energy of a neuron with similar firing mode, four distinct energy levels or footsteps can be detected when a neuron is excited to present four different firing activities [51]. A chaotic pattern often occupies a lower energy level, and periodic pattern often occupies a higher energy level. Both spiking and bursting can be considered as similar to quasi-periodic state, because distinct periodicity often requires higher energy level for keeping periodic oscillation.

For complete showing the dynamics of neural activities in a neuron model, oscillator like or map type, reproduction of

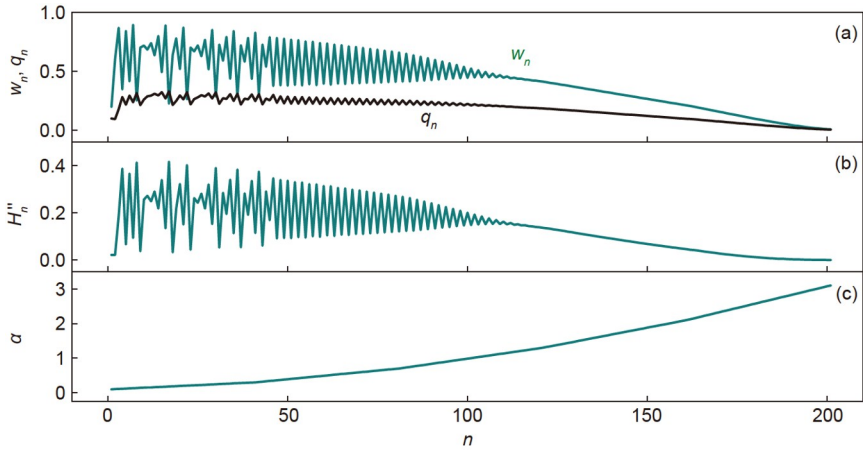

Figure 8 Evolution of variable w_n,q_n (a), Hamiltonian energy (b), and growth of memristive parameter α (c). Setting parameters α_0=0.1, β=0.01, κ= 0.5, η=3.9, p=1, μ=0.22. Average energy value finds 0.142.

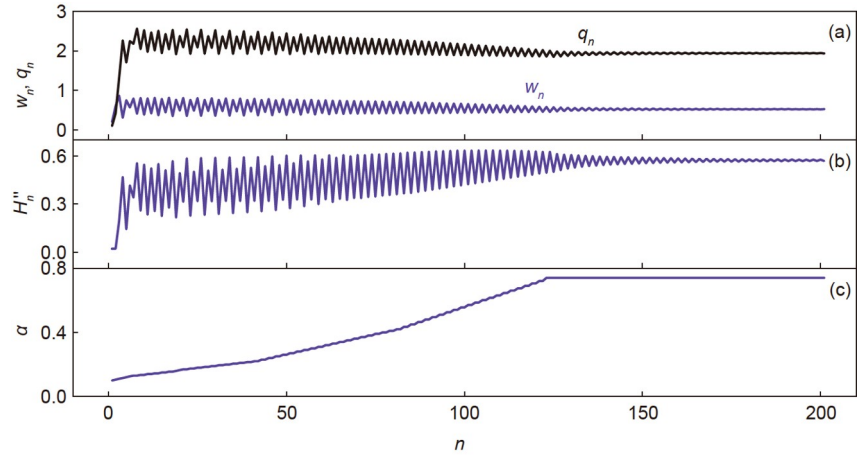

Figure 9 Evolution of variable w_n,q_n (a), Hamiltonian energy (b), and growth of memristive parameter α (c). Setting parameters α_0= 0.1, β=0.01, κ= 0.5, η=3.9, p=1, μ=1.85. Average energy value finds 0.502.

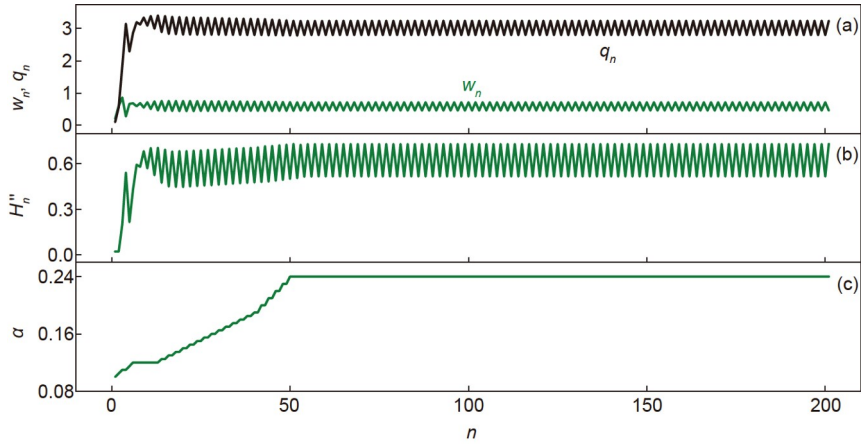

Figure 10 Evolution of variable w_n,q_n (a), Hamiltonian energy (b), and growth of memristive parameter α (c). Setting parameters α_0= 0.1, β=0.01, κ= 0.5, η=3.9, p=1, μ=2.58. Average energy value finds 0.607.

complete firing modes is the main characteristic. In presence of noisy excitation, nonlinear resonances can be induced by taming the intensity of noisy disturbance. Besides the calculation of *SNR* (signal to noise ratio) and *CV* (coefficient variability) vs. noise intensity, the distribution of average Hamilton energy <*H*> with different noise intensities provides a more effective way to predict the emergence of coherence resonance. Within a transient period or iterations *N*,

average energy <H> prefers to estimate the average power of the neuron or nonlinear oscillator, and high energy level is effective to keep distinct periodic state. Therefore, noise excitation can be applied on the right side of the first formula in eqs. (4) and (14). By taming the noise intensity, similar coherence resonance can be induced and confirmed by estimating the distribution of CV values or <H_n> for eqs. (21) and (22). The Hamilton energy function H can be used as Lyapunov function, dH/dτ often means energy release and the system becomes stable within finite transient period. The discrete energy function H_n is effective to restrict the stability in a map. When energy is released in stable way, H_n is decreased in each iteration, and then

$$\frac{H_{n+1}-H_n}{H_n-H_{n-1}}<1\ . \tag{24}$$

In the last decades, more interesting works about computational neuroscience have been finished on neuron models presented in nonlinear oscillators [62–65], some of which are included with biophysical effects, and numerical approach of membrane potentials for neurons and further statistical analysis often involves reliability of numerical algorithm in presence of noisy disturbance. Based on these oscillator-like models, coupling channels and links are tamed to control the collective behaviors in networks with linear, hybrid and higher order interaction [66–70], respectively. Map approach from equivalent nonlinear oscillator and nonlinear circuits, and reliability verification of the proposed maps can find clues from the scheme in this paper. In particular, energy definition for maps becomes helpful to discern the dependence of oscillatory modes on energy level provides new insights to predict occurrence of nonlinear resonance and further control under energy flow.

4 Conclusions

In this work, physical approach of an oscillator neuron with memristive term is discussed, and the equivalent nonlinear circuits are suggested to mimic the nonlinear terms and neural activities in the memristive neuron. It suggests two kinds of neural circuits by using different functional electric components. That is, a memristive oscillator can be implemented in some equivalent circuits composed of different electric components. When capacitive component as capacitor is not available, a CCM can behave similar role for supporting energy exchange between magnetic field and electric field. In particular, linear transition of sampled variables from the memristive oscillator and accompanying with time scale (such as time step for the nonlinear oscillator) can define a group of new variables, which are combined to build function maps. It provides theoretical evidence and guidance to design functional maps rather than giving mathematical maps arbitrarily. The obtained functional maps have good covariant feature with the original functional oscillators. For example, removing the subscript for the variables in the map will show the same form in the formula for nonlinear oscillator. As a result, a suitable energy function with the same weight for capacitive, inductive and memristive terms can be obtained for the memristive map in theoretical way. We also suggest an adaptive law to control one memristive parameter in the map under energy flow, mode transition occurs accompanying with energy shift during the mode transition. It explains the self-adaption property in map neurons from energy aspect. For further application of digital circuits and intelligent computation based on maps, readers can refer to this work and then some feasible maps can be designed from physical aspect. The suggested functional maps can be used for exploring pattern stability and wave propagation in the networks composed of maps [71–74]. The scheme throws insights on the study the maps coupled with discrete memristor [75–80]. The scheme is also helpful for presenting reliable map neurons and further application of setting map networks. Memristive terms accounts for the emergence of multistability and coexistence of more attractors, and it also provides energy source for some controllable neural circuits and biological neurons [81,82]. It is worthy of investigating the collective behaviors and self-organization of networks composed of reliable neurons, and thus researchers can find bridges to discover the potential dynamical mechanism for some neural disease [83,84].

This work was supported by the National Natural Science Foundation of China (Grant No. 12072139).

1 Heinrich M, Dahms T, Flunkert V, et al. Symmetry-breaking transitions in networks of nonlinear circuit elements. New J Phys, 2010, 12: 113030
2 Kenkel S W, Straley J P. Percolation theory of nonlinear circuit elements. Phys Rev Lett, 1982, 49: 767–770
3 Sivaganesh G, Srinivasan K, Arulgnanam A. Analytical studies on the dynamics of higher-dimensional nonlinear circuit systems. Pramana, 2022, 96: 185
4 Ardila V, Ramirez F, Suarez A. Analytical and numerical bifurcation analysis of circuits based on nonlinear resonators. IEEE Trans Microwave Theor Techn, 2021, 69: 4392–4405
5 Gao X, Mou J, Xiong L, et al. A fast and efficient multiple images encryption based on single-channel encryption and chaotic system. Nonlinear Dyn, 2022, 108: 613–636
6 Xin J, Hu H, Zheng J. 3D variable-structure chaotic system and its application in color image encryption with new Rubik's Cube-like permutation. Nonlinear Dyn, 2023, 111: 7859–7882
7 Ning X, Dong Q, Zhou S, et al. Construction of new 5D Hamiltonian conservative hyperchaotic system and its application in image encryption. Nonlinear Dyn, 2023, 111: 20425–20446
8 Liu X, Tong X, Wang Z, et al. Construction of controlled multi-scroll conservative chaotic system and its application in color image encryption. Nonlinear Dyn, 2022, 110: 1897–1934
9 Wang R, Wang Y, Xu X, et al. Brain works principle followed by neural information processing: A review of novel brain theory. Artif Intell Rev, 2023, 56: 285–350
10 Quaranta G, Lacarbonara W, Masri S F. A review on computational

intelligence for identification of nonlinear dynamical systems. Nonlinear Dyn, 2020, 99: 1709–1761
11 Groschner L N, Malis J G, Zuidinga B, et al. A biophysical account of multiplication by a single neuron. Nature, 2022, 603: 119–123
12 Tagluk M E, Isik I. Communication in nano devices: Electronic based biophysical model of a neuron. Nano Commun Netw, 2019, 19: 134–147
13 Wu F Q, Ma J, Zhang G. Energy estimation and coupling synchronization between biophysical neurons. Sci China Tech Sci, 2020, 63: 625–636
14 Clark R, Fuller L, Platt J A, et al. Reduced-dimension, biophysical neuron models constructed from observed data. Neural Comput, 2022, 34: 1545–1587
15 Sotero R C, Trujillo-Barreto N J. Biophysical model for integrating neuronal activity, EEG, fMRI and metabolism. NeuroImage, 2008, 39: 290–309
16 Ma J. Biophysical neurons, energy, and synapse controllability: A review. J Zhejiang Univ Sci A, 2023, 24: 109–129
17 Wu F Q, Guo Y T, Ma J. Energy flow accounts for the adaptive property of functional synapses. Sci China Tech Sci, 2023, 66: 3139–3152
18 Yang F, Xu Y, Ma J. A memristive neuron and its adaptability to external electric field. Chaos-An Interdisciplinary J NOnlinear Sci, 2023, 33: 023110
19 Xie Y, Yao Z, Ma J. Formation of local heterogeneity under energy collection in neural networks. Sci China Tech Sci, 2023, 66: 439–455
20 Yang F, Wang Y, Ma J. Creation of heterogeneity or defects in a memristive neural network under energy flow. Commun NOnlinear Sci Numer Simul, 2023, 119: 107127
21 Real E, Asari H, Gollisch T, et al. Neural circuit inference from function to structure. Curr Biol, 2017, 27: 189–198
22 Pan Y, Monje M. Activity shapes neural circuit form and function: A historical perspective. J Neurosci, 2020, 40: 944–954
23 Davis F P, Nern A, Picard S, et al. A genetic, genomic, and computational resource for exploring neural circuit function. eLife, 2020, 9: e50901
24 Sussillo D. Neural circuits as computational dynamical systems. Curr Opin Neurobiol, 2014, 25: 156–163
25 Wu F, Yao Z. Dynamics of neuron-like excitable Josephson junctions coupled by a metal oxide memristive synapse. Nonlinear Dyn, 2023, 111: 13481–13497
26 Xie Y, Yao Z, Hu X, et al. Enhance sensitivity to illumination and synchronization in light-dependent neurons. Chin Phys B, 2021, 30: 120510
27 Zhou P, Yao Z, Ma J, et al. A piezoelectric sensing neuron and resonance synchronization between auditory neurons under stimulus. Chaos Solitons Fractals, 2021, 145: 110751
28 Xu Y, Liu M, Zhu Z, et al. Dynamics and coherence resonance in a thermosensitive neuron driven by photocurrent. Chin Phys B, 2020, 29: 098704
29 Tagne J F, Edima H C, Njitacke Z T, et al. Bifurcations analysis and experimental study of the dynamics of a thermosensitive neuron conducted simultaneously by photocurrent and thermistance. Eur Phys J Spec Top, 2022, 231: 993–1004
30 Zhu Z, Ren G, Zhang X, et al. Effects of multiplicative-noise and coupling on synchronization in thermosensitive neural circuits. Chaos Solitons Fractals, 2021, 151: 111203
31 Shen H, Yu F, Wang C, et al. Firing mechanism based on single memristive neuron and double memristive coupled neurons. Nonlinear Dyn, 2022, 110: 3807–3822
32 Wu F, Hu X, Ma J. Estimation of the effect of magnetic field on a memristive neuron. Appl Math Comput, 2022, 432: 127366
33 Wen Z, Wang C, Deng Q, et al. Regulating memristive neuronal dynamical properties via excitatory or inhibitory magnetic field coupling. Nonlinear Dyn, 2022, 110: 3823–3835
34 Xu Q, Ju Z, Ding S, et al. Electromagnetic induction effects on electrical activity within a memristive Wilson neuron model. Cogn Neurodyn, 2022, 16: 1221–1231
35 Kafraj M S, Parastesh F, Jafari S. Firing patterns of an improved Izhikevich neuron model under the effect of electromagnetic induction and noise. Chaos Solitons Fractals, 2020, 137: 109782
36 Narayanan R, Johnston D. Functional maps within a single neuron. J Neurophysiol, 2012, 108: 2343–2351
37 Ibarz B, Casado J M, Sanjuán M A F. Map-based models in neuronal dynamics. Phys Rep, 2011, 501: 1–74
38 Muni S S, Fatoyinbo H O, Ghosh I. Dynamical effects of electromagnetic flux on chialvo neuron map: Nodal and network behaviors. Int J Bifurcation Chaos, 2022, 32: 2230020
39 Ramakrishnan B, Mehrabbeik M, Parastesh F, et al. A new memristive neuron map model and its network's dynamics under electrochemical coupling. Electronics, 2022, 11: 153
40 Bao H, Li K X, Ma J, et al. Memristive effects on an improved discrete Rulkov neuron model. Sci China Tech Sci, 2023, 66: 3153–3163
41 Li Y, Wang Z, Midya R, et al. Review of memristor devices in neuromorphic computing: Materials sciences and device challenges. J Phys D-Appl Phys, 2018, 51: 503002
42 Khalid M. Review on various memristor models, characteristics, potential applications, and future works. Trans Electr Electron Mater, 2019, 20: 289–298
43 Thakkar P, Gosai J, Gogoi H J, et al. From fundamentals to frontiers: A review of memristor mechanisms, modeling and emerging applications. J Mater Chem C, 2024, 12: 1583–1608
44 Lin H, Wang C, Deng Q, et al. Review on chaotic dynamics of memristive neuron and neural network. Nonlinear Dyn, 2021, 106: 959–973
45 Lai Q, Lai C. Design and implementation of a new hyperchaotic memristive map. IEEE Trans Circuits Syst II, 2022, 69: 2331–2335
46 Liu X, Sun K, Wang H, et al. A class of novel discrete memristive chaotic map. Chaos Solitons Fractals, 2023, 174: 113791
47 Ramadoss J, Almatroud O A, Momani S, et al. Discrete memristance and nonlinear term for designing memristive maps. Symmetry, 2022, 14: 2110
48 Rong K, Bao H, Li H, et al. Memristive Hénon map with hidden Neimark–Sacker bifurcations. Nonlinear Dyn, 2022, 108: 4459–4470
49 Bao B, Zhao Q, Yu X, et al. Complex dynamics and initial state effects in a two-dimensional sine-bounded memristive map. Chaos Solitons Fractals, 2023, 173: 113748
50 Fox R F, Gatland I R, Roy R, et al. Fast, accurate algorithm for numerical simulation of exponentially correlated colored noise. Phys Rev A, 1988, 38: 5938–5940
51 Li X, Xu Y. Energy level transition and mode transition in a neuron. Nonlinear Dyn, 2024, 112: 2253–2263
52 Mantegna R N. Fast, accurate algorithm for numerical simulation of Lévy stable stochastic processes. Phys Rev E, 1994, 49: 4677–4683
53 Guo Y, Xie Y, Ma J. How to define energy function for memristive oscillator and map. Nonlinear Dyn, 2023, 111: 21903–21915
54 Ma J. Energy function for some maps and nonlinear oscillators. Appl Math Comput, 2024, 463: 128379
55 Isah A, Bilbault J M. Review on the basic circuit elements and memristor interpretation: Analysis, technology and applications. J Low Power Electron Appl, 2022, 12: 44
56 Abraham I. The case for rejecting the memristor as a fundamental circuit element. Sci Rep, 2018, 8: 10972
57 Ramakrishnan B, Durdu A, Rajagopal K, et al. Infinite attractors in a chaotic circuit with exponential memristor and Josephson junction resonator. AEU-Int J Electron Commun, 2020, 123: 153319
58 Isah A, Nguetcho A S T, Binczak S, et al. Dynamics of a charge-controlled memristor in master–slave coupling. Electron Lett, 2020, 56: 211–213
59 Sun J, Yang J, Liu P, et al. Design of general flux-controlled and charge-controlled memristor emulators based on hyperbolic functions. IEEE Trans Comput-Aided Des Integr Circuits Syst, 2022, 42: 956–967
60 Sharma P K, Ranjan R K, Khateb F, et al. Charged controlled mem-

element emulator and its application in a chaotic system. IEEE Access, 2020, 8: 171397–171407
61 Wang C, Tang J, Ma J. Minireview on signal exchange between nonlinear circuits and neurons via field coupling. Eur Phys J Spec Top, 2019, 228: 1907–1924
62 Wang X, Yu D, Wu Y, et al. Effects of potassium channel blockage on inverse stochastic resonance in Hodgkin-Huxley neural systems. J Zhejiang Univ Sci A, 2023, 24: 735–748
63 Huang W, Yang L, Zhan X, et al. Synchronization transition of a modular neural network containing subnetworks of different scales. Front Inform Technol Electron Eng, 2023, 24: 1458–1470
64 Xie Y, Yao Z, Ma J. Phase synchronization and energy balance between neurons. Front Inform Technol Electron Eng, 2022, 23: 1407–1420
65 Wu F, Gu H, Jia Y. Bifurcations underlying different excitability transitions modulated by excitatory and inhibitory memristor and chemical autapses. Chaos Solitons Fractals, 2021, 153: 111611
66 Majhi S, Perc M, Ghosh D. Dynamics on higher-order networks: A review. J R Soc Interface, 2022, 19: 20220043
67 Li X, Ghosh D, Lei Y. Chimera states in coupled pendulum with higher-order interaction. Chaos Solitons Fractals, 2023, 170: 113325
68 Parastesh F, Mehrabbeik M, Rajagopal K, et al. Synchronization in Hindmarsh–Rose neurons subject to higher-order interactions. Chaos-An Interdiscipl J Nonlinear Sci, 2022, 32: 013125
69 Ramasamy M, Devarajan S, Kumarasamy S, et al. Effect of higher-order interactions on synchronization of neuron models with electromagnetic induction. Appl Math Comput, 2022, 434: 127447
70 Kundu S, Ghosh D. Higher-order interactions promote chimera states. Phys Rev E, 2022, 105: L042202
71 Atay F M, Jost J, Wende A. Delays, connection topology, and synchronization of coupled chaotic maps. Phys Rev Lett, 2004, 92: 144101
72 Koronovskii A A, Moskalenko O I, Shurygina S A, et al. Generalized synchronization in discrete maps. New point of view on weak and strong synchronization. Chaos Solitons Fractals, 2013, 46: 12–18
73 Winkler M, Sawicki J, Omelchenko I, et al. Relay synchronization in multiplex networks of discrete maps. Europhys Lett, 2019, 126: 50004
74 Muni S S, Rajagopal K, Karthikeyan A, et al. Discrete hybrid Izhikevich neuron model: Nodal and network behaviours considering electromagnetic flux coupling. Chaos Solitons Fractals, 2022, 155: 111759
75 Ma M, Yang Y, Qiu Z, et al. A locally active discrete memristor model and its application in a hyperchaotic map. Nonlinear Dyn, 2022, 107: 2935–2949
76 Peng Y, He S, Sun K. A higher dimensional chaotic map with discrete memristor. AEU-Int J Electron Commun, 2021, 129: 153539
77 Zhong H, Li G, Xu X. A generic voltage-controlled discrete memristor model and its application in chaotic map. Chaos Solitons Fractals, 2022, 161: 112389
78 Ren L, Mou J, Banerjee S, et al. A hyperchaotic map with a new discrete memristor model: Design, dynamical analysis, implementation and application. Chaos Solitons Fractals, 2023, 167: 113024
79 Bao H, Hua Z Y, Liu W B, et al. Discrete memristive neuron model and its interspike interval-encoded application in image encryption. Sci China Tech Sci, 2021, 64: 2281–2291
80 Li C, Yang Y, Yang X, et al. Application of discrete memristors in logistic map and Hindmarsh–Rose neuron. Eur Phys J Spec Top, 2022, 231: 3209–3224
81 Bao H, Chen Z G, Cai J M, et al. Memristive cyclic three-neuron-based neural network with chaos and global coexisting attractors. Sci China Tech Sci, 2022, 65: 2582–2592
82 Lu L L, Yi M, Liu X Q. Energy-efficient firing modes of chay neuron model in different bursting kinetics. Sci China Tech Sci, 2022, 65: 1661–1674
83 Yuan Y Y, Yang H, Han F, et al. Traveling chimera states in locally coupled memristive Hindmarsh-Rose neuronal networks and circuit simulation. Sci China Tech Sci, 2022, 65: 1445–1455
84 Yu Y, Fan Y B, Han F, et al. Transcranial direct current stimulation inhibits epileptic activity propagation in a large-scale brain network model. Sci China Tech Sci, 2023, 66: 3628–3638